Volume 4 | Number 5 | May 2017 | Pages 985–1200

Environmental Science
Nano

rsc.li/es-nano

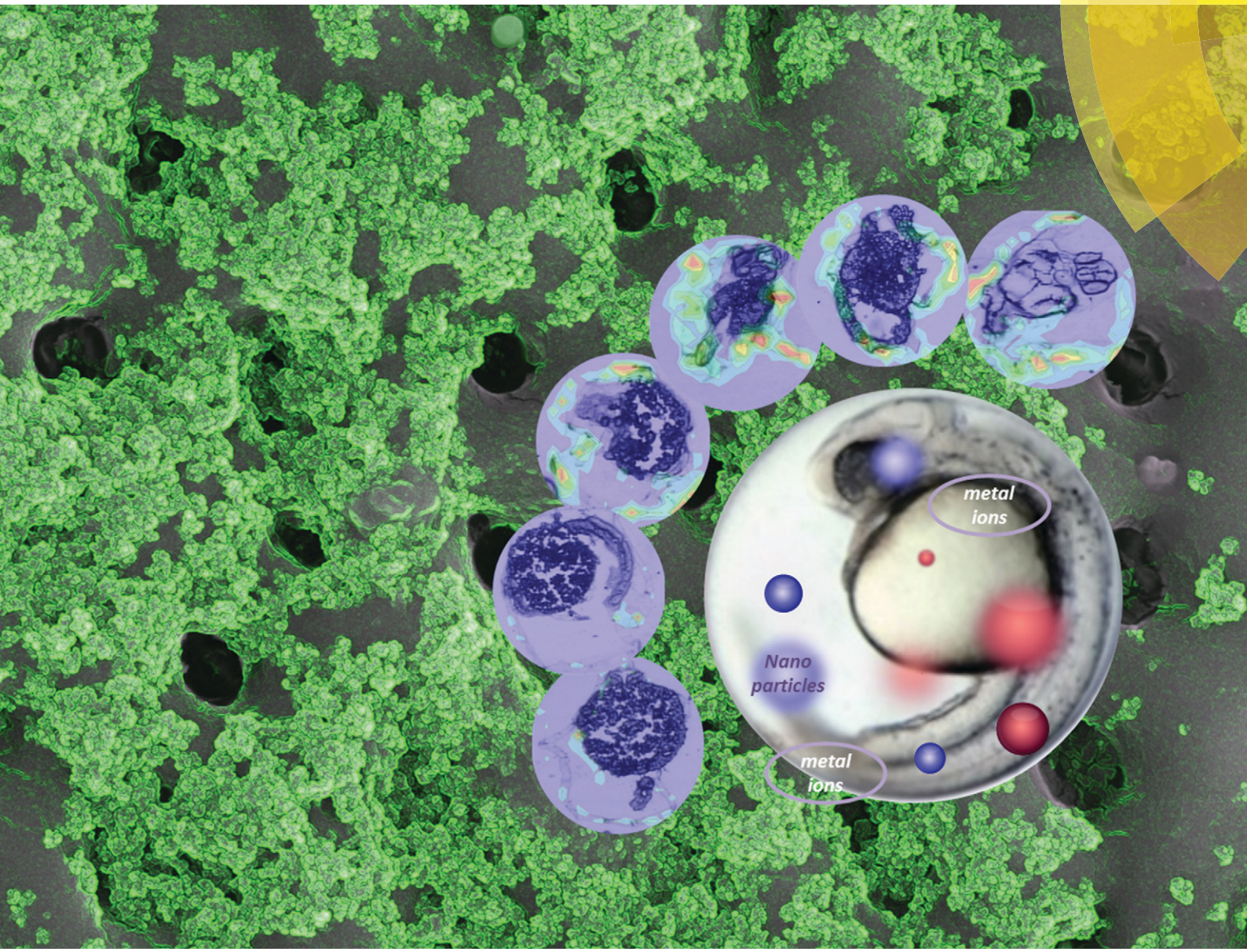

ISSN 2051-8153

ROYAL SOCIETY OF CHEMISTRY

PAPER
Dana Kühnel *et al.*
Metal uptake and distribution in the zebrafish (*Danio rerio*) embryo: differences between nanoparticles and metal ions

Environmental Science Nano

PAPER

View Article Online
View Journal | View Issue

Cite this: *Environ. Sci.: Nano*, 2017, 4, 1005

Metal uptake and distribution in the zebrafish (*Danio rerio*) embryo: differences between nanoparticles and metal ions†

Steffi Böhme,‡[a] Marta Baccaro,§[b] Matthias Schmidt,[c] Annegret Potthoff,[d] Hans-Joachim Stärk,[e] Thorsten Reemtsma[e] and Dana Kühnel*[a]

Received 28th September 2016,
Accepted 5th March 2017

DOI: 10.1039/c6en00440g

rsc.li/es-nano

The zebrafish (*Danio rerio*) embryo (ZFE) is an established test organism for investigating the toxicity of chemicals and is suitable for the assessment of the hazardous potential of nanoparticles. There is little knowledge on metal internalization and distribution in these organisms, as well as on the underlying kinetic processes. To shed light on metal–ZFE interactions, the uptake of different metal-composed nanoparticles (Ag-, Au-, CuO-, ZnO-NP) and their dissolved cations was studied in terms of temporal and spatial distribution as well as internal concentrations considering different ZFE compartments (whole egg, embryo, chorion, perivitelline space). By applying laser ablation ICP-MS and electron microscopy, element-specific differences in metal distribution at the surface and within the test organisms were observed. As determined by nebulization ICP-MS, all metals showed a bioconcentration in the eggs. Gold showed the highest accumulation, followed by silver, zinc and copper, with distinct differences when comparing the uptake of nanoparticles and metal ions. Upon exposure to nanoparticles, more silver and zinc were detected in the organisms, whereas more copper accumulated upon exposure to the cations. For silver, gold, and copper, the major share was found at the chorion structures, irrespective of exposure to NPs or cations. In contrast, for zinc, the highest portion reached the inner embryo. Overall, our results provide an informative basis to explain the differences in nanoparticle and ion toxicity observed in various studies.

Environmental significance

The aim of this work was to explore the association and internalization of nanomaterials with the test organism zebrafish embryo. There is little knowledge in general on metal internalization and distribution in these organisms, as well as on the underlying kinetic processes. For 4 different metals, distribution and uptake in zebrafish embryos is reported. Quantitative data on nanoparticle and cation uptake are compared in a compartment-specific way and distinct differences between the metals and the type of metal representation were identified. This is the first study assessing metal accumulation in embryonic zebrafish, an important alternative animal model in human and ecotoxicology. Hence, these results are considered of high importance for the elucidation of nanoparticle-specific effects as well as for future toxicokinetic studies.

Introduction

The zebrafish (*Danio rerio*) embryo (ZFE) toxicity test is a versatile *in vitro* method to assess the hazard of chemicals and has been applied in several studies for the toxicological testing of nanoparticles (NPs) (*e.g.* ref. 1–4). The ZFE as a vertebrate model species combines advantages such as rapid development and transparency of embryos and is considered as an alternative model to animals for testing.[5] It allows the observation of lethal, acute, and sublethal toxicological endpoints.[6]

[a] *Department of Bioanalytical Ecotoxicology, Helmholtz Centre for Environmental Research - UFZ, Permoserstrasse 15, 04318 Leipzig, Germany. E-mail: dana.kuehnel@ufz.de*
[b] *Department of Physical Sciences, Earth and Environment, University of Siena, Via Mattioli 4, 53100 Siena, Italy*
[c] *Department of Isotope Biogeochemistry, Helmholtz Centre for Environmental Research - UFZ, Permoserstrasse 15, 04318 Leipzig, Germany*
[d] *Department of Powder and Suspension Characterization, Fraunhofer Institute for Ceramic Technologies and Systems - IKTS, Winterbergstrasse 28, 01277 Dresden, Germany*
[e] *Department of Analytical Chemistry, Helmholtz Centre for Environmental Research - UFZ, Permoserstrasse 15, 04318 Leipzig, Germany*

† Electronic supplementary information (ESI) available: Additional information is available. Table S1: Comparison of nominal and measured exposure concentrations. Table S2: Control values (neb-ICP-MS). Table S3: Nanoparticle characteristics. Table S4: Percentage distribution and concentrations for the ZFE egg, chorion, and embryo. Table S5: Internal concentrations. Fig. S1: Control values (LA-ICP-MS). Fig. S2: Visualization of time course of metal accumulation to ZFE. See DOI: 10.1039/c6en00440g

‡ Current address: RIKILT (Wageningen University & Research Centre), Akkermaalsbos 2, 6708 WB Wageningen, The Netherlands.
§ Current address: Division of Toxicology, Wageningen University, Stippeneng 4, 6708 WE Wageningen, The Netherlands.

To estimate the toxic potency of organic substances, it is essential to determine both the internal dose and the velocity of uptake, which trigger the occurrence of effects.[7] Internal concentrations of organic compounds internalized by ZFE were successfully correlated to toxicological effects.[8–10] However, for metal toxicity, not only the internalized but also the attached fraction may affect organisms. But little knowledge on the uptake of metals by ZFE and the underlying kinetic processes exists.[11] For metal-based nanoparticles, it is expected that their distribution follows a temporal and spatial pattern different from that of dissolved chemical substances, such as metal ions.[12,13] Data on the association of NPs with the ZFE are scarce, with regard to both the quantification of internalized amounts and the visualization of particle distribution. For both, analytical methods need optimization, in order to combine high sensitivity and high spatial resolution to detect NPs within biological tissues.[14] In recent studies, mainly electron microscopy (SEM, TEM),[15,16] fluorescence microscopy,[17,18] and laser ablation inductively coupled plasma mass spectrometry (LA-ICP-MS)[2,3,19,20] were applied to detect nanomaterials in cells and organisms.

In terms of metal and metal oxide distribution, different compartments of the embryo were considered. Specific attention was paid to the role of the chorion, a specific structure protecting the embryo from external influences until hatching, but at the same time being permeable enough to allow sufficient gas supply and advective transport of nutrients for the embryo.[21] The surface charge of the chorion is described as negative,[22] attracting and binding positively charged metal ions.[23] The chorion is traversed by pore channels with a diameter of ~200 nm.[22] As such, its barrier function will impact the internalization of metals and metal ions, and its permeability for ions will probably differ from that for particles. However, for Zn^{2+} and nanoscale ZnO, no differences in the uptake and tissue distribution in embryos and eleutheroembryos were observed.[2] In previous studies, the passage of NPs through the chorion but also retention on its surface were reported. The direct passage of Au-NPs (~12 nm) and stabilized Ag-NPs (5–20 nm) through the chorion pore channels was demonstrated.[24,25] In contrast, the retention of Ag-NPs and TiO_2-NPs at the chorion was also observed.[26,27] A barrier function of the chorion was likewise reported for several other NPs, namely Ru@SiO_2 particles (60, 200 nm),[17] as well as CuO-, ZnO-, Co_3O_4-, and NiO-NPs (all NPs with a primary particle size of 20–50 nm).[18] Furthermore, Auffan *et al.* (2014)[28] concluded that the chorion acts as a protective membrane limiting the internalization of NPs as well as metal cations.

The aim of this study was to gain novel knowledge on the time-dependent interaction between ZFE and metal-based NPs and metal cations. ZFE were exposed to non-toxic concentrations of the NPs (Ag-, Au-, CuO-, and ZnO) and corresponding cations (Cu^{2+}, Ag^{+} and Zn^{2+} ions) for different periods of time (0.5, 1, 2, 4, 8, and 24 h). The specific objectives were (1) the quantification of metal/metal oxide associated with or internalized in different compartments of the ZFE (chorion, embryo), (2) the visualization of distribution patterns, and (3) a kinetic study of metal/metal oxide attachment at or within the ZFE chorion structures. The metal internalization was compared for the different materials as well as for the two exposure regimes, NPs or cations in order to assess whether differences in the kinetic processes occur.

Materials and methods

Characterization of nanoparticle powders, suspensions, and exposure solutions

The nanoparticles (Au-, Ag-, ZnO-, CuO-NPs) were provided and characterized in detail by project partners of the EU project NanoValid. The Ag- and Au-NPs were delivered as water-based suspensions stabilized with polyvinyl pyrrolidone (PVP) and sodium citrate, respectively, to prevent agglomeration processes within the suspension. The CuO- and ZnO-NPs were provided as powders. The CuO-NPs were stabilized by the addition of 0.1% tetrasodium pyrophosphate and sonicated according to an established protocol.[29] As no suitable stabilizer was found for the ZnO-NPs, a 10 g l^{-1} stock suspension was sonicated in deionized water and left for 24 h, and the resulting supernatant (~80%) was taken as a nanoscale fraction for the following characterization and biological experiments. The stock suspensions were further diluted to the respective test concentrations in the test medium used for the zebrafish embryo test, referred to as ISO water (294.0 mg l^{-1} $CaCl_2{\cdot}2H_2O$, 123.3 mg l^{-1} $MgSO_4{\cdot}7H_2O$, 63.0 mg l^{-1} $NaHCO_3$, and 5.5 mg l^{-1} KCl dissolved in deionized water[30]).

The properties and characteristics of the four NPs, namely the primary particle size, the specific surface area (BET), the particle size distribution as well as the zeta potential in the stock suspensions, are listed in the ESI.† Furthermore, the stability and agglomeration behavior of particles in the exposure suspensions were investigated by dynamic light scattering (DLS). The dissolved ionic fraction within the NP exposure suspensions was measured prior to testing by ICP-MS in the supernatant after 30 min of centrifugation at 16 000*g*. For the NP exposure, it has to be pointed out that the suspensions contained dissolved metal cations besides the metal (oxide) NPs (except for Au-NPs).

Metal salts

In parallel to the NPs, with the exception of Au, all experiments were performed with the respective metal salt solutions ($AgNO_3$, $CuSO_4{\cdot}5H_2O$, $ZnSO_4{\cdot}7H_2O$; Merck). The Au-NPs are inert and no release of ions is expected, therefore the respective salt was not tested. For each salt, stock solutions in deionized water were prepared, which were further diluted to the respective test concentrations in ISO water.[30] For $CuSO_4{\cdot}5H_2O$, the stock concentration was 2 g l^{-1}, for $AgNO_3$ 100 mg l^{-1} and for $ZnSO_4{\cdot}7H_2O$ 426 mg l^{-1}.

Upon dissolution in zebrafish culture medium, different metal species will be present in the exposure solutions. However, as metal speciation was not further differentiated in this study, the term cation is used in the following.

Zebrafish maintenance, embryo exposure, and sample preparation

Zebrafish (*Danio rerio*) embryos (ZFE) were exposed to the respective NPs and metal ions according to the OECD test guideline 236 (6). Fish were maintained at 26 ± 1 °C in a 14 h : 10 h light : dark cycle and fed daily with *Artemia* sp. For the egg collection, spawn traps were placed into the fish tanks on the day prior to spawning. The institution has all relevant permissions to breed zebrafish (Federal State of Saxony, Landesdirection Sachsen, license number DD24-5131/252/7). All experiments involving zebrafish embryos were performed in compliance with the relevant laws and institutional guidelines. After the selection of fertilized eggs, exposure experiments were started at 26 hours post fertilization (hpf) in ISO water for different time periods (0.5, 1, 2, 4, 8, and 24 h). For every 70 ml of exposure solution, 35 eggs (making 2 ml per egg) were incubated in petri dishes with one individual metal (in the form of either NPs or ions). No mixtures of metals were tested. The organisms were kept at 26 ± 1 °C, with no change of medium during the exposure. Before the onset of exposure, the pH of ISO water was adjusted to 7.8 ± 0.2. The organisms were exposed to 60 μg element per l of NPs since this concentration reflects environmentally relevant concentrations[31] and exerted no toxicological effects for any of the applied NPs. For the metal salt solutions, likewise 60 μg element per l were used to assess the impact of the dissolved ionic fraction.

Elemental concentrations were measured by ICP-MS from a 1 mL volume of the exposure suspensions prior to testing (Table S1†). After exposure, only undamaged, living organisms were collected and washed in medium (ISO water) twice to remove loosely bound particles. Afterwards, the concentrations of the respective metals were determined in the whole ZFE (referred to as "egg"), isolated chorion (referred to as chorion), or isolated inner embryo (referred to as inner embryo). The chorion and embryo were separated mechanically by using forceps. For the quantification of internalized metal, 4 of the respective organism compartments were pooled to obtain one sample and a minimum of 3 replicates were used for analysis. For the visualization of the elemental distribution by LA-ICP-MS, exposed organisms were fixated, embedded in frozen section medium and cut in 40 μm sections using a microtome at −20 °C as described previously.[19,20]

Quantification of total elemental concentrations

For analysis of the total elemental concentrations in exposed organisms, samples were subjected to 2 h of acid digestion (DigiPrep, S-Prep) at 95 °C to generate homogeneous solutions. The acid digestion protocol was adjusted to the physico-chemical properties of the individual NPs and metal salts. Samples exposed to Ag- and Cu (NPs or metal salt) were digested with nitric acid (65%, suprapur, Merck), and those exposed to Au- and Zn (NPs or metal salt) were digested with *aqua regia* (v/v HCl/HNO_3, 3/1). The digested samples were subsequently analyzed by a quadrupole-based (ELAN DRCe, Perkin Elmer Sciex) nebulization ICP-MS method (neb-ICP-MS) to determine the elemental concentrations. An external calibration was performed by analyzing elemental standard reference solutions. For all experiments, untreated organisms were used as negative controls (blank) (Fig. S1, Table S2†) and the blank concentrations (natural background) were subtracted from the concentrations measured in the exposed organisms. The natural backgrounds of the respective elements in unexposed zebrafish embryos were determined as follows: silver (0.1 ng per organism), gold (0.2 ng per organism), zinc (2.7 ng per organism) and copper (1.8 ng per organism). The latter background values were well in line with those of Bourassa *et al.* (2014)[32] (Table S2, Fig. S1†).

The metal content of the perivitelline space (PVS), which could not be sampled individually, was calculated by subtracting the chorion and embryo concentrations from the total amount determined for the egg.

Visualization by laser ablation ICP-MS

The organism sections placed on glass slides were introduced into an ablation chamber and ablated by a Nd:YAG laser with a wavelength of 266 nm (LSX 500, CETAC). The laser energy was adjusted to 60% to ensure complete ablation of the organic layer. The spot ablation was performed with a 50 μm spot diameter for sufficient imaging. The generated particle aerosol was directly transported and introduced into the ICP-MS *via* an additional argon gas stream. The external calibration was performed by the laser ablation ICP-MS (LA-ICP-MS) measurement of individually particle-spiked agarose gels according to an earlier protocol.[33] The transient intensity signals for the individual spots were collected in a data matrix, transformed to concentration values by using the calibration curves and plotted as 2D-colored images.[20] For all experiments, untreated organisms were measured as controls (blank) (Fig. S2†). For Ag and Au, the natural background was below the detection limit (for limits of detection, see Böhme *et al.*, 2015[20]). In contrast, for Zn and Cu, a higher natural abundance was observed and thus the blank intensities were subtracted from the sample intensities to obtain the final images.

Analysis of particle distribution by scanning electron microscopy

In order to confirm the NP localization determined by LA-ICP-MS and to gain more detailed insights into the localization of the particles at or within the chorion structure, organisms exposed for 24 h were subjected to electron microscopy. The organisms were washed and fixated as mentioned above, placed on SEM-stubs with an adhesive carbon foil and dried at room temperature for 2 h. In order to increase the conductivity, a 10 nm chromium layer was inductively sputtered onto the biological samples. Chromium was chosen instead of the commonly used Au/Pd because its X-ray lines are well separated from those of Au, Ag, Cu, and Zn, respectively. The samples were subsequently investigated using a scanning electron microscope (SEM, Zeiss Merlin VP compact)

equipped with an energy-dispersive X-ray spectroscopy detector (EDX detecting unit, Bruker Quantax) for elemental analysis. With respect to the X-ray lines, the following accelerating voltages were applied for the respective elements: 2.5 (Au-, CuO-NPs), 3.0 (ZnO-NPs), 4.5 (Ag-NPs), and 5 kV for controls.

Data evaluation and statistics

For the calculation of the distribution of the metal over the different compartments, the mass-based values measured after 8 and 24 h exposure time were used. Average values (mean ± SD) of three independent experiments for each of the two time points were obtained. For the calculation of the elemental concentrations per compartment, the volume of each compartment was determined by microscopic inspection of 24 hpf eggs. A total volume of ~700 nl was calculated for the egg from the diameter of 1100 μm by assuming a spherical shape. According to Rawson *et al.* (2000),[34] the thickness of the chorion is ~2 μm, resulting in a volume of 8 nl. The embryo and yolk had a volume of 220 nl, leaving ~472 nl for the PVS. The concentration for each element per compartment (in ng μl^{-1}) was calculated by dividing the average mass after 8 and 24 h of exposure by the volume of the respective compartment.

For the comparison of uptake kinetics upon exposure to particles or ions, the elemental mass (in ng) per compartment was plotted for each time point, and a *t*-test was performed to determine significant differences between the particle and ion exposure in terms of elemental mass associated with the respective compartment of the ZFE.

All analyses were performed with Microsoft Excel 2016 (Microsoft Corporation, Redmond, USA), OriginLab 8 (ADDITIVE GmbH, Friedrichsdorf, Germany) and GraphPad Prism 4 (GraphPad Software Inc., La Jolla, CA), and all graphs were prepared using GraphPad Prism 4.

Results & discussion

Characterization of nanoparticle powders, stock and exposure suspensions

The primary characterization data are provided in the ESI† (Table S3). Briefly, the primary particle sizes of the selected NPs are in the range of 10–25 nm. The hydrodynamic particle sizes measured in the ISO-water exposure suspensions at the start of the experiments were as follows: 18 ± 2 nm (Au-NPs), 80 ± 1 nm (ZnO-NPs), 117 ± 24 nm (Ag-NPs), and 132 ± 2 nm (CuO-NPs). After 24 h of exposure, sizes of 204 nm (Ag-NPs), 420 nm (CuO-NPs), and >5 μm for Au- and ZnO-NPs were measured, indicating strong agglomeration of particles within the media.

For the majority of the NP exposure suspensions, a difference between the nominal (applied) and measured elemental concentrations was observed at the start of each experiment (Table S1†). The dissolved fraction of the respective particle exposure suspensions was determined to be 48 ± 7% Ag (Ag-NPs), 10 ± 5% Cu (CuO-NPs), and 58 ± 3% Zn (ZnO-NPs) at the beginning of the experiment. High amounts of dissolved ions within the media were previously reported with values of 20–53% for ZnO-NPs and 12–38% for Ag-NPs.[2,35] The continuous release of ions from the NP surface can lead to total NP dissolution as described for ZnO-NPs.[36,37] The dissolution of ZnO-NPs reflects the higher solubility of ZnO in comparison to the other materials studied, *e.g.* CuO,[38] and we expect an increase of the dissolved Zn proportion or even total particle dissolution until the end of the exposure time of 24 h, as for these particles no stabilizer was used. Further, our results for copper dissolution (10 ± 5%) are well in line with those of Lin *et al.* (2013)[39] and Hua *et al.* (2014)[40] who also reported a dissolved fraction of around 10%. The dissolution process is assumed to be dynamic over time and depends on factors such as particle concentration, size, medium composition, pH, and the presence of organisms.[37,41,42] As a consequence, upon exposure to either Ag-NPs, ZnO-NPs or CuO-NPs, zebrafish embryos were exposed to the respective metal ions in addition to the nanoparticles. Hence, both the visualization and the quantification data represent a mixture of NPs and ions, as the origin of the element cannot be differentiated between particulate or ionic. However, based on the dissolution data, we assume an increasing contribution of the particles to the total amount of internalized metal in the order of ZnO-NP (high share of ions) < Ag-NP < CuO-NP (high share of particles) < Au-NP (only particulate) exposure.

Distribution of NPs and metals in different ZFE compartments

After exposure to 60 μg element per l for different durations, the metal uptake and distribution (from either NP or cation exposure) within the ZFE was analyzed by LA-ICP-MS and visualized by the reconstruction of color maps according to Böhme *et al.* (2015).[20] Color maps showing the elemental distribution in ZFE exposed to either nanoparticles or ions for different time points (0.5 to 24 h) are shown in Fig. S2.†

As shown in Fig. 1a, Ag-NPs strongly associate with the chorion and substantial amounts seem to reach the PVS, whereas only minor amounts reach the embryo. A high sorption of Ag-NPs to the chorion structure was previously reported and quantified by Auffan *et al.* (2014)[28] with a percentage of 58 to 85% Ag-NPs accumulating at the chorion after 48 h of exposure to 5 mg l^{-1} Ag-NPs. Ionic silver stemming from the $AgNO_3$ solution was predominantly located in the PVS and to a lesser extent in the chorion (Fig. 1a).

Gold nanoparticles (Fig. 1d) show a distribution comparative to Ag-NPs, with most material found at the chorion and in the PVS, but only little material located in the inner embryo.

After exposure to nanoparticles, copper was detected on the chorion and in the embryo. After exposure to copper cations, only very little copper was detected in the embryo and a larger fraction at the chorion (Fig. 2a). For both exposure regimes, minor amounts were calculated for the PVS. For CuO-NPs, however, the color maps (Fig. 2c) do not well represent the accumulation patterns determined by neb-ICP-MS. Neither accumulation at the chorion nor a clear increase in metal concentrations for the inner embryo can be observed.

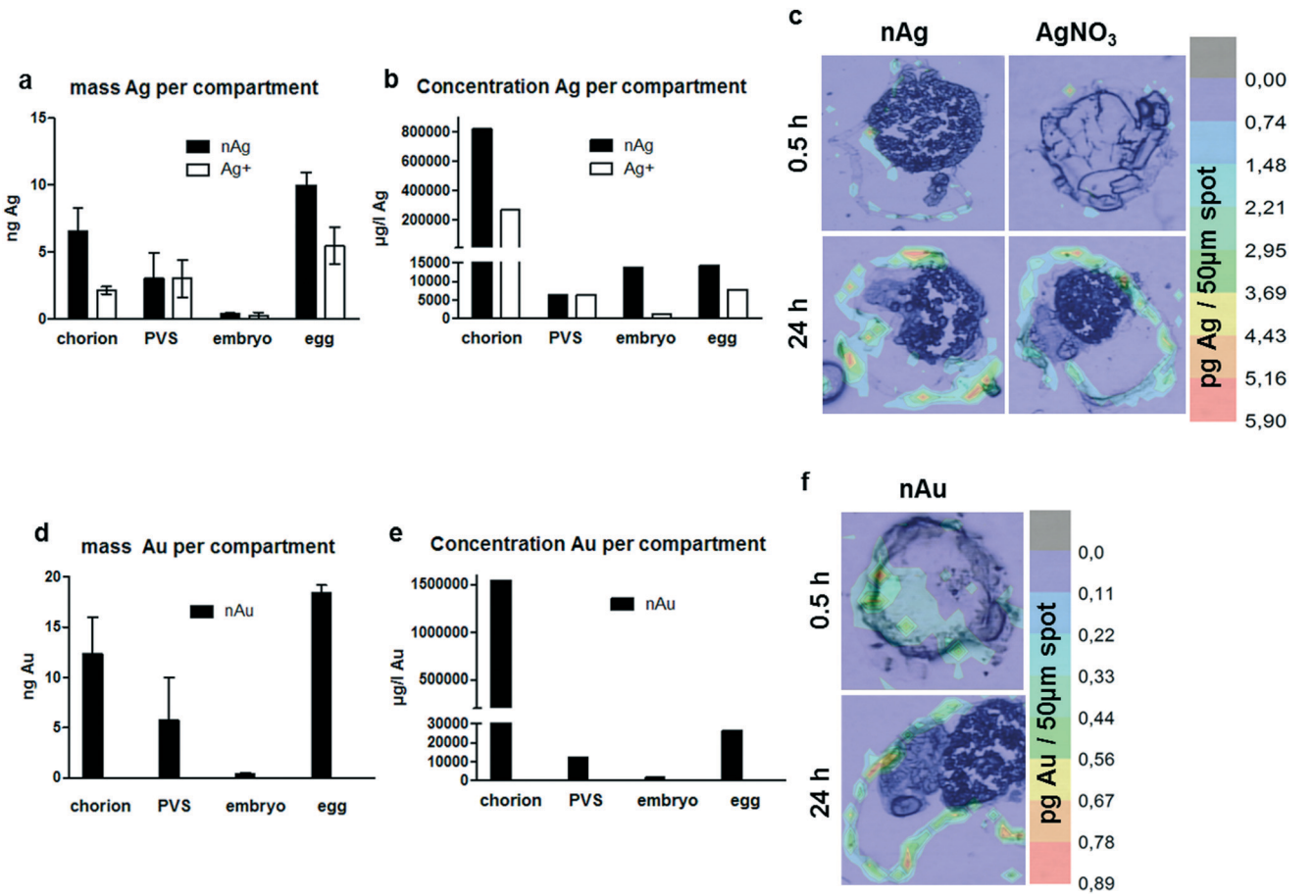

Fig. 1 Distribution (a and d) and concentration (b and e) of silver (a and b) and gold (d and e) in zebrafish embryos after exposure to nanoparticles (black bars) and metal ions (white bars, only silver). Average values (mean ± SD from 3 independent replicates) of the respective masses (in ng per compartment) detected after 8 and 24 h of exposure were calculated. The graphs depict the mass and the concentrations of the respective element allocated to the different compartments of the embryo (chorion, PVS, embryo, whole egg). Note the individual scaling of the *y*-axes. The color panels (c and f) show the distribution of the respective metal as reconstructed after LA-ICP-MS measurements taken after 0.5 (start of exposure) and 24 h (end of exposure). The color index indicates the amount of element detected in the respective area from red (high concentration) to blue (low concentration).

This may be due to the LA-ICP-MS method, which is a semi-quantitative imaging technique that records elemental distributions for only one thin section of the whole organism.

Of the four elements studied, zinc showed the most exceptional distribution pattern, with the largest fraction detected in the inner embryo, irrespective of whether the embryos were exposed to the nanoparticles or the cations. Strikingly, only minor amounts were found to accumulate at the chorion. More zinc accumulated in the PVS upon exposure to the nanoparticles (Fig. 2d). These results are well in line with the observation made by Brun *et al.* (2014)[2] for ionic and particulate zinc with high Zn concentrations detected for the embryo. As in this study dechorionated embryos for the visualization of Zn distribution were used, a direct comparison with the distributions patterns observed in this study is not possible. With regard to copper and gold distribution in fish embryos (NPs and ions), no data are available so far in the literature.

To explore the role of the chorion in metal retention or transport in more detail, scanning electron microscopy was applied. Besides the observation of the sorption and agglomeration behavior of the NPs at the ZFE chorion structures, the specific aim was to shed light on the role of the pore channels in nanoparticle uptake. All types of NPs (Ag-, Au-, CuO-, ZnO-NPs) were detected at the chorion surface and their chemical identity was verified by EDX mapping and the measurement of EDX spectra for the respective elements (Fig. 3). In addition, for Au- and CuO-NPs, particle agglomeration was observed in selected regions of interest. However, the Ag- and ZnO-NPs were more difficult to identify in the particulate state, probably due to their high dissolution rates. Rather, these two elements were found to be homogeneously distributed over the entire chorion surface. We were not able to assess the presence of NPs in the pore channels or the association of particles with other chorion structures by this method.

Quantification of NPs and metals in different ZFE compartments

The quantification of metal concentrations in different ZFE compartments by neb-ICP-MS revealed element-specific

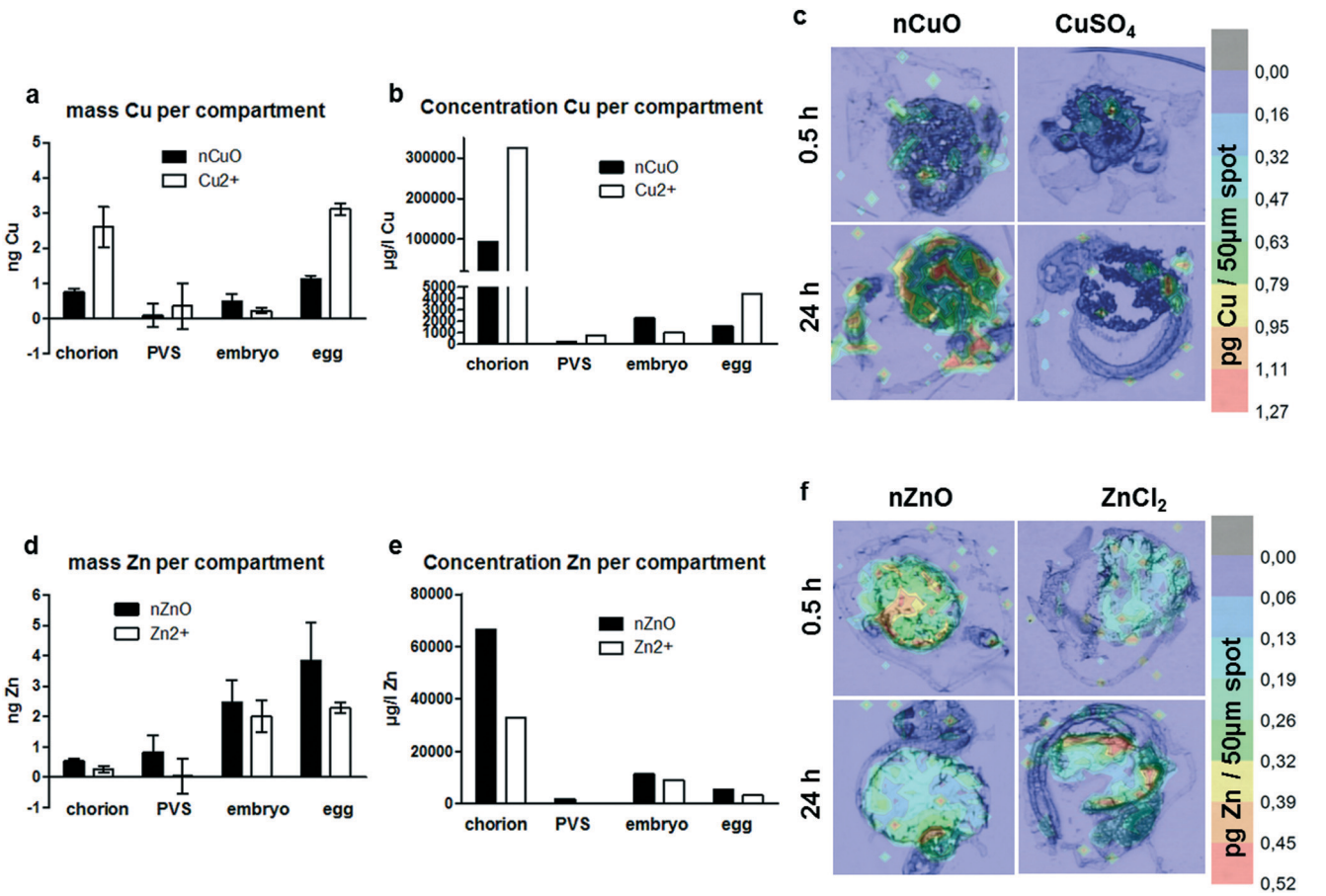

Fig. 2 Distribution (a and d) and concentration (b and e) of copper (a and b) and zinc (d and e) in zebrafish embryos after exposure to nanoparticles (black bars) and metal ions (white bars). Average values (mean ± SD from 3 independent replicates) of the respective masses (in ng per compartment) detected after 8 and 24 h of exposure were calculated. The graphs depict the distribution and the concentrations of the respective element in the different compartments of the embryo (chorion, PVS, embryo, whole egg). Note the individual scaling of the *y*-axes. The color panels (c and f) show the distribution of the respective metal as reconstructed after LA-ICP-MS measurements taken after 0.5 (start of exposure) and 24 h (end of exposure). The color index indicates the amount of element detected in the respective area from red (high concentration) to blue (low concentration).

differences in the uptake behavior depending on how elements were presented to the organisms (as cations or NPs). Despite showing comparable distribution patterns, both the absolute and the internal metal concentrations measured for the corresponding ions differ from those of the nanoparticles (Fig. 1 and 2). The concentrations of Ag, Au, Cu and Zn determined for each ZFE compartment after exposure to nanoparticles and cations (from 0.5 to 24 h) are listed in Table S4.†

More material associated with the organism upon Ag-NP exposure compared to cation exposure. In detail, Ag-NPs showed a high presence at the chorion (24 h: 5.6 ng Ag per chorion) (Fig. 4a–c). Minor concentrations were detected in the inner embryo for both Ag- and Au-NP exposure (24 h: <0.3 and 0.4 ng per embryo, respectively). Distinct, significant differences in silver uptake were observed when comparing particle and cation exposure. For the whole egg as well as the chorion, significantly more silver associated with the compartments after exposure to nanoparticles (24 h: 10 and 6.5 ng per egg, and 5.6 and 2.2 ng Ag per chorion for Ag-NPs and Ag cations, respectively) (Fig. 4a and b). No significant differences between particle and cation exposure were observed in the embryo and the PVS (Fig. 1a and 3c). Expressed in percentages, ~65% of the Ag-NPs and 67% of the Au-NPs detected on the whole egg associated with the chorion. For Ag-NPs, this is well in line with the observation of Auffan *et al.* (2014),[28] who reported that 58 to 85% of Ag-NPs accumulate at the chorion of Atlantic killifish embryos depending on medium salinity. The use of NP stabilizers seems to have a minor influence on the uptake behavior, as Auffan *et al.* (2014)[28] used citrate-stabilized Ag-NPs, and also the uptake of uncoated Ag-NPs was reported.[43]

Of all metals investigated, gold nanoparticles showed the highest amount associating with zebrafish eggs, with 24.8 ng per organism after 24 h exposure time, with most metal found associated with the chorion (24 h: 18.9 ng per chorion) (-Fig. 4d–f). Minor concentrations were detected in the inner embryo (24 h: 0.4 ng per embryo). Expressed in percentages, 67% of the Au-NPs detected on the whole egg associated with the chorion. Browning *et al.* (2009, 2013)[44,45] demonstrated likewise the uptake of non-stabilized Au-NPs into the inner mass

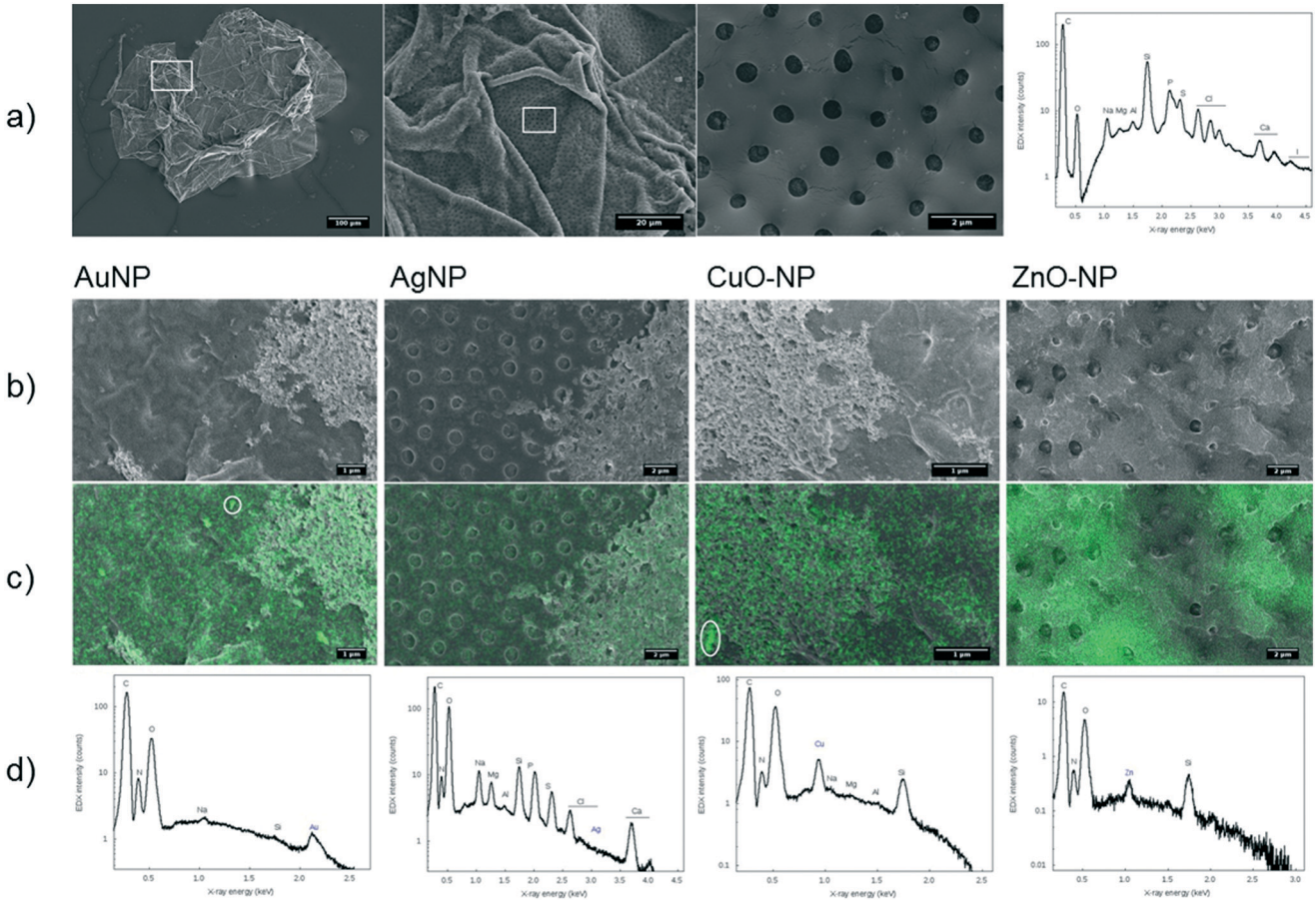

Fig. 3 SEM + EDX investigations at the ZFE chorion surface with a) representative images and spectra of the control (untreated chorion). Electron microscopy pictures for each NP (b), overlay with the EDX map of the respective element (c), and the EDX spectra (d) for the whole area (Ag-, ZnO-NPs) or for selected regions of interest (Au-, CuO-NPs) are shown.

of zebrafish embryos, however, no direct comparison regarding the internalized mass of the Au-NPs to our data is possible.

Copper showed less association with the zebrafish egg compared to silver and gold, with maximum values <4 ng per organism (Fig. 2 and 4). Copper showed the highest accumulation at the chorion (24 h: 2.7 and 1.1 ng Cu per chorion for NPs and cations, respectively) and accordingly at the whole egg (24 h: 1.5 and 3.3 ng Cu per egg for NPs and cations, respectively) (Fig. 2a, 4g and h). For the CuO-NPs, ~67% of the total amount of the element found in the fish egg associated with the chorion, which is, however, not well supported by the visualization data, probably due to the lower sensitivity of the LA-ICP-MS compared to the neb-ICP-MS. As a unique feature for this element, cation exposure resulted in significantly higher internalization of copper than NP exposure. This is well in agreement with recent data for juvenile trout gill, showing that the accumulation of Cu is greater from $CuSO_4$ than from Cu-NPs.[46] In addition, as observed for silver, a higher share of copper was translocated to the PVS upon exposure to the cations, possibly due to facilitated transport of ions through the chorion. Hence, our data do not support the modelling results from Muller *et al.* (2015)[47] and Hua *et al.* (2014),[40] which predicted that eight times more Cu accumulates in the PVS upon exposure to nanoparticles compared to ions. However, one has to keep in mind that particle transport across the chorion may depend on particle size as well as additional particle properties such as surface coatings or stabilizers. As different types of CuO-NPs were used in the study by Hua *et al.* (2014)[40] and this study, a direct comparison may not be possible.

Interestingly, a clear difference in zinc uptake occurred between particles and cations even though a high dissolution rate was found for the particles. Zinc displayed a unique pattern of accumulation, in that only very little material was detected at the chorion (24 h: 0.4 and 0.07 ng Zn per chorion for NP and cation exposure, respectively), with most material reaching the inner embryo (24 h: 2.4 ng Zn per embryo for NP and cation exposure) (Fig. 2d and e; Fig. 4k and l). In the PVS, more Zn was detected upon exposure to NPs (Fig. 2d). Interestingly, the calculation of element content revealed that less zinc allocates to the PVS than to the embryo (Fig. 2, Table S4†). For Zn-NPs, ~64% of the total material was detected in the inner embryo, which matches the elemental distribution observed by LA-ICP-MS. These amounts are in agreement with the quantitative results of Brun *et al.* (2014),[2] showing dose-dependent zinc accumulation for the embryo (~80%)

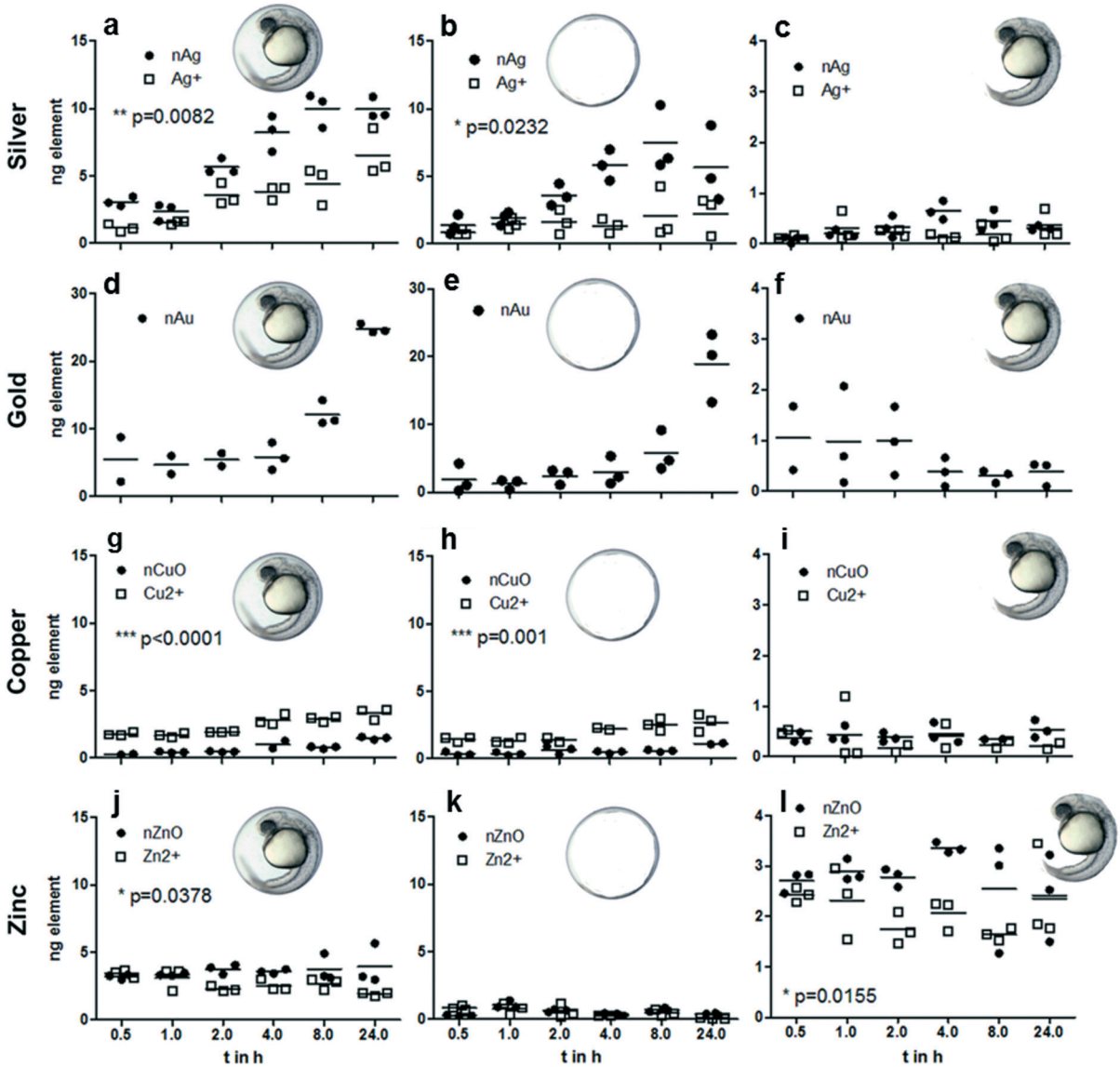

Fig. 4 Time-resolved data for elemental concentrations in ZFE after exposure to 60 μg l^{-1} NPs ($n \geq 3$, shown as mean ± SD) for silver (a–c), gold (d–f), copper (g–i) and zinc (j–l). Different compartments were considered: left – whole egg, middle – chorion, right – embryo only. Significant differences in element content upon exposure to nanoparticles (●) and metal ions (□) were analyzed by a *t*-test and are indicated by * ($p < 0.05$), ** ($p < 0.005$) or *** ($p < 0.001$). Note the individual scaling of the *y*-axes.

after 48 and 96 h of exposure with up to 5 mg l^{-1} ZnO-NPs. Contrary to the ZnO-NPs used in our study, the positively charged ZnO-NPs used by Brun *et al.* (2014)[2] were stabilized by the addition of negatively charged alginate, yet, comparable uptake of Zn into the embryo was observed.

By taking the respective ZFE compartment volumes into account, for each metal and compartment, internal concentrations were calculated. All of the metals showed a bioconcentration in all compartments considered, as all internal concentrations were above the external exposure concentrations (valid for both nominal and real concentrations in the exposure medium, see Table S1†). The strong enrichment of metals at the chorion was confirmed for all metals except Zn cations, with concentrations of 66 000 (nZnO)–1 545 000 (nAu) μg l^{-1} (Fig. 1b and e, Fig. 2b and e and Table S5†).

These results show for the first time that significant differences in association and internalization of nanoparticles and cations occur. This outcome is even more striking when the dissolution of ions from the nanoparticles selected for this study is considered. Due to this, during the nanoparticle exposure, the ZFE were exposed simultaneously to particles as well as ions, but still a clear effect of the particulate fraction was obvious.

Time-dependent internalization of metals into different ZFE compartments

To date, quantitative data showing the association of metals with zebrafish embryos over time are scarce. Hence, the distribution and uptake of metals (either from NP or cation

exposure) into different compartments of the ZFE was determined by neb-ICP-MS after exposure to 60 μg element per l after different exposure durations (0.5, 1, 2, 4, 8 and 24 h). To our knowledge, this is the first study assessing the time course in such detail.

The kinetic data demonstrate a steady increase in the elemental concentrations associated with the organisms during the time of observation, irrespective of exposure to NPs or cations (Fig. 4). Considering the whole egg, for silver, gold and copper, no apparent saturation after 24 h exposure time is observed (Fig. 4a, d and g). For Cu and Zn, after 0.5 h, almost the total concentration detected after 24 h exposure duration is associated with the eggs (Fig. 4g and j). However, it has to be noted that the zinc concentrations remain rather constant over time, and for the cation exposure, a tendency for a decrease of zinc concentrations in the whole egg and embryo is observed. As the same observation is made for copper accumulation in the embryo, one can hypothesize that this distribution pattern is influenced by transport processes regulating the internal concentration of these essential trace elements in zebrafish embryos.[48–50] An interesting observation was made for the gold content of embryos, which seems to decrease over time (Fig. 4f). Browning *et al.* (2009, 2013)[44,45] demonstrated the passive diffusion of Au-NPs into the inner mass of the embryo, however, in their studies the gold stayed in the embryo for an observation time of up to 120 h.

Conclusion

In summary, our results show that the type of metal seems to be crucial for the amount of metal associated with the zebrafish eggs. Our results demonstrate an element-specific distribution of metal over the different zebrafish embryo compartments. As demonstrated by the internal concentrations, a bioconcentration of all metals inside the embryo was observed.

The dosage form (NPs or cations) causes clearly identifiable, but smaller differences in adsorption and uptake. Hence, our results support the assumption that differences between NPs and the corresponding ions as observed in several nanotoxicity studies may be explainable based on the differences in the uptake kinetics or the time course of association with the organisms.[35,51] An influence of the stabilizers used for the NPs cannot be excluded, but is considered to be weak. Particle-related properties such as hydrodynamic diameter, dissolution or surface charge do not correlate directly with the uptake by the embryo, but this requires confirmation using a larger data set.

For future studies, the discrimination of internalized NPs *versus* ions would allow one to shed more light on the influence of kinetic processes on toxic effects. Therefore, analytical techniques have to be developed further to differentiate between the internalization and distribution of particles or ions. At first, this requires imaging methods with a spatial resolution significantly higher than that provided by LA-ICP-MS Furthermore, the role of the local enrichment of nanoparticles at certain structures of organisms, and the continuous dissolution processes during exposure and after internalization by organisms need further clarification, with a specific focus on the chorion structure in the case of ZFE.

Acknowledgements

This research was funded by the EU FP7 project NanoValid (Development of reference methods for hazard identification, risk assessment and LCA of engineered nanomaterials; grant no. 263147). The authors thank Josefine Müller of the Department of Bioanalytical Ecotoxicology (UFZ) for her help in the laboratory. The analytical facilities of the Centre for Chemical Microscopy (ProVIS) at the Helmholtz Centre for Environmental Research were supported by the European Regional Development Funds (EFRE–Europe Funds Saxony) and the Helmholtz Association.

References

1 P. V. Asharani, L. W. Yi, Z. Y. Gong and S. Valiyaveettil, Comparison of the toxicity of silver, gold and platinum nanoparticles in developing zebrafish embryos, *Nanotoxicology*, 2011, **5**(1), 43–54.
2 N. R. Brun, M. Lenz, B. Wehrli and K. Fent, Comparative effects of zinc oxide nanoparticles and dissolved zinc on zebrafish embryos and eleuthero-embryos: Importance of zinc ions, *Sci. Total Environ.*, 2014, **476**, 657–666.
3 D. Chen, D. Zhang, C. Y. Jimmy and K. M. Chan, Effects of Cu 2 O nanoparticle and CuCl 2 on zebrafish larvae and a liver cell-line, *Aquat. Toxicol.*, 2011, **105**(3), 344–354.
4 M. Weil, T. Meißner, W. Busch, A. Springer, D. Kühnel, R. Schulz and K. Duis, The oxidized state of the nanocomposite Carbo-Iron® causes no adverse effects on growth, survival and differential gene expression in zebrafish, *Sci. Total Environ.*, 2015, **530–531**, 198–208.
5 S. Scholz, S. Fischer, U. Gündel, E. Küster, T. Luckenbach and D. Voelker, The zebrafish embryo model in environmental risk assessment—applications beyond acute toxicity testing, *Environ. Sci. Pollut. Res.*, 2008, **15**(5), 394–404.
6 OECD, *Test No. 236: Fish Embryo Acute Toxicity (FET) Test*, www.oecd.org, 2013.
7 B. I. Escher and J. L. Hermens, Peer reviewed: internal exposure: linking bioavailability to effects, *Environ. Sci. Technol.*, 2004, **38**(23), 455A–462A.
8 S. Brox, A. P. Ritter, E. Küster and T. Reemtsma, A quantitative HPLC–MS/MS method for studying internal concentrations and toxicokinetics of 34 polar analytes in zebrafish (Danio rerio) embryos, *Anal. Bioanal. Chem.*, 2014, **406**(20), 4831–4840.
9 S. El-Amrani, J. Sanz-Landaluze, J. Guinea and C. Camara, Rapid determination of polycyclic aromatic hydrocarbons (PAHs) in zebrafish eleutheroembryos as a model for the evaluation of PAH bioconcentration, *Talanta*, 2013, **104**, 67–74.

10 A. Kühnert, C. Vogs, R. Altenburger and E. Küster, The internal concentration of organic substances in fish embryos—a toxicokinetic approach, *Environ. Toxicol. Chem.*, 2013, **32**(8), 1819–1827.

11 R. Redelstein, H. Zielke, D. Spira, U. Feiler, L. Erdinger, H. Zimmer, S. Wiseman, M. Hecker, J. P. Giesy, T. B. Seiler and H. Hollert, Bioaccumulation and molecular effects of sediment-bound metals in zebrafish embryos, *Environ. Sci. Pollut. Res.*, 2015, **22**(21), 16290–16304.

12 A. Praetorius, N. Tufenkji, K. U. Goss, M. Scheringer, F. von der Kammer and M. Elimelech, The road to nowhere: equilibrium partition coefficients for nanoparticles, *Environ. Sci.: Nano*, 2014, **1**(4), 317–323.

13 J. Wang and W. X. Wang, Significance of physicochemical and uptake kinetics in controlling the toxicity of metallic nanomaterials to aquatic organisms, *J. Zhejiang Univ., Sci., A*, 2014, **15**(8), 573–592.

14 B. J. Marquis, S. A. Love, K. L. Braun and C. L. Haynes, Analytical methods to assess nanoparticle toxicity, *Analyst*, 2009, **134**(3), 425–439.

15 P. Asharani, Y. L. Wu, Z. Gong and S. Valiyaveettil, Toxicity of silver nanoparticles in zebrafish models, *Nanotechnology*, 2008, **19**(25), 1–8.

16 M. Heinlaan, A. Kahru, K. Kasemets, B. Arbeille, G. Prensier and H. C. Dubourguier, Changes in the Daphnia magna midgut upon ingestion of copper oxide nanoparticles: A transmission electron microscopy study, *Water Res.*, 2011, **45**(1), 179–190.

17 K. Fent, C. J. Weisbrod, A. Wirth-Heller and U. Pieles, Assessment of uptake and toxicity of fluorescent silica nanoparticles in zebrafish (Danio rerio) early life stages, *Aquat. Toxicol.*, 2010, **100**(2), 218–228.

18 S. Lin, Y. Zhao, T. Xia, H. Meng, Z. Ji, R. Liu, S. George, S. Xiong, X. Wang, H. Zhang, S. Pokhrel, L. Mädler, R. Damoiseaux, S. Lin and A. E. Nel, High Content Screening in Zebrafish Speeds up Hazard Ranking of Transition Metal Oxide Nanoparticles, *ACS Nano*, 2011, **5**(9), 7284–7295.

19 S. Böhme, H.-J. Stärk, T. Reemtsma and D. Kühnel, Effect propagation after silver nanoparticle exposure in zebrafish (Danio rerio) embryos: a correlation to internal concentration and distribution patterns, *Environ. Sci.: Nano*, 2015, **2**(6), 603–614.

20 S. Böhme, H. J. Stark, D. Kuhnel and T. Reemtsma, Exploring LA–ICP–MS as a quantitative imaging technique to study nanoparticle uptake in *Daphnia magna* and zebrafish (Danio rerio) embryos, *Anal. Bioanal. Chem.*, 2015, **407**(18), 5477–5485.

21 D. M. Rawson, T. Zhang, D. Kalicharan and W. L. Jongebloed, Field emission scanning electron microscopy and transmission electron microscopy studies of the chorion, plasma membrane and syncytial layers of the gastrula-stage embryo of the zebrafish Brachydanio rerio: a consideration of the structural and functional relationships with respect to cryoprotectant penetration, *Aquacult. Res.*, 2000, **31**(3), 325–336.

22 N. H. Hart and M. Donovan, Fine structure of the chorion and site of sperm entry in the egg of Brachydanio, *J. Exp. Zool.*, 1983, **227**(2), 277–296.

23 K. Henn, Limits of the fish embryo toxicity test with Danio rerio as an alternative to the acute fish toxicity test, *Dissertation*, Ruperto-Carola University of Heidelberg, Germany, 2011.

24 L. M. Browning, K. J. Lee, T. Huang, P. D. Nallathamby, J. E. Lowman and X.-H. N. Xu, Random walk of single gold nanoparticles in zebrafish embryos leading to stochastic toxic effects on embryonic developments, *Nanoscale*, 2009, **1**(1), 138–152.

25 K. J. Lee, L. M. Browning, P. D. Nallathamby and X.-H. N. Xu, Study of charge-dependent transport and toxicity of peptide-functionalized silver nanoparticles using zebrafish embryos and single nanoparticle plasmonic spectroscopy, *Chem. Res. Toxicol.*, 2013, **26**(6), 904–917.

26 Y.-J. Shih, C.-C. Su, C.-W. Chen, C.-D. Dong, W.-S. Liu and C. P. Huang, Adsorption characteristics of nano-TiO2 onto zebrafish embryos and its impacts on egg hatching, *Chemosphere*, 2016, **154**, 109–117.

27 O. J. Osborne, B. D. Johnston, J. Moger, M. Balousha, J. R. Lead, T. Kudoh and C. R. Tyler, Effects of particle size and coating on nanoscale Ag and TiO(2) exposure in zebrafish (Danio rerio) embryos, *Nanotoxicology*, 2013, **7**(8), 1315–1324.

28 M. Auffan, C. W. Matson, J. Rose, M. Arnold, O. Proux, B. Fayard, W. Liu, P. Chaurand, M. R. Wiesner, J. Y. Bottero and R. T. Di Giulio, Salinity-dependent silver nanoparticle uptake and transformation by Atlantic killifish (Fundulus heteroclitus) embryos, *Nanotoxicology*, 2014, **8**, 167–176.

29 E.-p. NanoValid, *Dispersion of NNV-011 (CuO) nanoparticle suspensions for toxicological testing*, 2015.

30 ISO, International Standards, Water quality - Determination of the acute lethal toxicity of substances to a freshwater fish [Brachydanio rerio] Hamilton -Buchanan (Teleostei, Cyprinidae). ISO 7346-3: Flow-through method, International Organisation for Standardisation, 1996, Available: [http://www.iso.org].

31 T. Y. Sun, F. Gottschalk, K. Hungerbühler and B. Nowack, Comprehensive probabilistic modelling of environmental emissions of engineered nanomaterials, *Environ. Pollut.*, 2014, **185**, 69–76.

32 D. Bourassa, S. C. Gleber, S. Vogt, H. Yi, F. Will, H. Richter, C. H. Shin and C. J. Fahrni, 3D imaging of transition metals in the zebrafish embryo by X-ray fluorescence microtomography, *Metallomics*, 2014, **6**(9), 1648–1655.

33 S. Böhme, H.-J. Stärk, T. Meißner, A. Springer, T. Reemtsma, D. Kühnel and W. Busch, Quantification of Al2O3 nanoparticles in human cell lines applying inductively coupled plasma mass spectrometry (neb-ICP-MS, LA-ICP-MS) and flow cytometry-based methods, *J. Nanopart. Res.*, 2014, **16**(9), 1–15.

34 D. M. Rawson, T. Zhang, D. Kalicharan and W. L. Jongebloed, Field emission scanning electron microscopy and transmission electron microscopy studies of the chorion, plasma membrane and syncytial layers of the gastrula-stage embryo of the zebrafish Brachydanio rerio: a consideration of the structural and functional relationships with respect to cryoprotectant penetration, *Aquacult. Res.*, 2000, **31**(3), 325–336.

35 J. Wang and W.-X. Wang, Significance of physicochemical and uptake kinetics in controlling the toxicity of metallic nanomaterials to aquatic organisms, *J. Zhejiang Univ., Sci., A*, 2014, **15**(8), 573–592.

36 S. Lopes, F. Ribeiro, J. Wojnarowicz, W. Łojkowski, K. Jurkschat, A. Crossley, A. M. Soares and S. Loureiro, Zinc oxide nanoparticles toxicity to Daphnia magna: size-dependent effects and dissolution, *Environ. Toxicol. Chem.*, 2014, **33**(1), 190–198.

37 N. Odzak, D. Kistler, R. Behra and L. Sigg, Dissolution of metal and metal oxide nanoparticles in aqueous media, *Environ. Pollut.*, 2014, **191**, 132–138.

38 Y.-N. Chang, M. Zhang, L. Xia, J. Zhang and G. Xing, The toxic effects and mechanisms of CuO and ZnO nanoparticles, *Materials*, 2012, **5**(12), 2850–2871.

39 S. Lin, Y. Zhao, Z. Ji, J. Ear, C. H. Chang, H. Zhang, C. Low-Kam, K. Yamada, H. Meng, X. Wang, R. Liu, S. Pokhrel, L. Mädler, R. Damoiseaux, T. Xia, H. A. Godwin, S. Lin and A. E. Nel, Zebrafish High-Throughput Screening to Study the Impact of Dissolvable Metal Oxide Nanoparticles on the Hatching Enzyme, ZHE1, *Small*, 2013, **9**(9–10), 1776–1785.

40 J. Hua, M. G. Vijver, F. Ahmad, M. K. Richardson and W. J. G. M. Peijnenburg, Toxicity of different-sized copper nano- and submicron particles and their shed copper ions to zebrafish embryos, *Environ. Toxicol. Chem.*, 2014, **33**(8), 1774–1782.

41 D. He, J. J. Dorantes-Aranda and T. D. Waite, Silver nanoparticle-algae interactions: oxidative dissolution, reactive oxygen species generation and synergistic toxic effects, *Environ. Sci. Technol.*, 2012, **46**(16), 8731–8738.

42 A. R. Harmon, A. J. Kennedy, A. R. Poda, A. J. Bednar, M. A. Chappell and J. A. Steevens, Determination of nanosilver dissolution kinetics and toxicity in an environmentally relevant aqueous medium, *Environ. Toxicol. Chem.*, 2014, **33**(8), 1783–1791.

43 K. J. Lee, L. M. Browning, P. D. Nallathamby, T. Desai, P. K. Cherukuri and X. H. N. Xu, In Vivo Quantitative Study of Sized-Dependent Transport and Toxicity of Single Silver Nanoparticles Using Zebrafish Embryos, *Chem. Res. Toxicol.*, 2012, **25**(5), 1029–1046.

44 L. M. Browning, K. J. Lee, T. Huang, P. D. Nallathamby, J. E. Lowman and X.-H. Nancy Xu, Random walk of single gold nanoparticles in zebrafish embryos leading to stochastic toxic effects on embryonic developments, *Nanoscale*, 2009, **1**(1), 138–152.

45 L. M. Browning, T. Huang and X.-H. N. Xu, Real-time in vivo imaging of size-dependent transport and toxicity of gold nanoparticles in zebrafish embryos using single nanoparticle plasmonic spectroscopy, *Interface Focus*, 2013, **3**(3), 20120098.

46 G. A. Al-Bairuty, D. Boyle, T. B. Henry and R. D. Handy, Sublethal effects of copper sulphate compared to copper nanoparticles in rainbow trout (Oncorhynchus mykiss) at low pH: physiology and metal accumulation, *Aquat. Toxicol.*, 2016, **174**, 188–198.

47 E. B. Muller, S. Lin and R. M. Nisbet, Quantitative Adverse Outcome Pathway Analysis of Hatching in Zebrafish with CuO Nanoparticles, *Environ. Sci. Technol.*, 2015, **49**(19), 11817–11824.

48 L. Zhao, Z. Xia and F. Wang, Zebrafish in the Sea of Mineral (Iron, Zinc and Copper) Metabolism, *Front. Pharmacol.*, 2014, **5**, 33.

49 Y. Jiang, S. Zhang, S. Feng, J. Sun and P. Xu, Genome Wide Identification, Phylogeny and Expression of Zinc Transporter Genes in Common Carp, *PLoS One*, 2015, **9**(12), e116043.

50 G. Yan, Y. C. Zhang, J. L. Yu, Y. Yu, F. Zhang, Z. Z. Zhang, A. M. Wu, X. H. Yan, Y. Zhou and F. D. Wang, Slc39a7/zip7 Plays a Critical Role in Development and Zinc Homeostasis in Zebrafish, *PLoS One*, 2012, **7**(8), e42939.

51 Y. Xiao, M. G. Vijver, G. Chen and W. J. G. M. Peijnenburg, Toxicity and Accumulation of Cu and ZnO Nanoparticles in Daphnia magna, *Environ. Sci. Technol.*, 2015, **49**(7), 4657–4664.